TopCAT – Topographical Compartment Analysis Tool to analyze seacliff and beach change in GIS

Michael J. Olsen[1], Adam P. Young[2], and Scott A. Ashford[1]*

1. School of Civil and Construction Engineering, Oregon State University
2. Scripps Institution of Oceanography, University of California, San Diego

corresponding author
220 Owen Hall
Corvallis, OR 97331
+1 (541)737-9327
Michael.olsen@oregonstate.edu

Abstract

This paper discusses the development of a new GIS extension named the Topographic Compartment Analysis Tool (*TopCAT*), which compares sequential digital elevation models (DEMs) and provides a quantitative and statistical analysis of the alongshore topographical change. *TopCAT* was specifically designed for the morphological analysis of seacliffs and beaches but may be applied to other elongated features which experience topographical change, such as stream beds, river banks, coastal dunes, etc. To demonstrate the capabilities of *TopCAT* two case studies are presented herein. The first case examines coastal cliff retreat for a 500 m section in Del Mar, California and shows that large failures comprised a large portion of the total eroded volume and the average retreat rate does not provide a good estimate of local maximum cliff retreat. The second case investigates the alongshore volumetric beach sand change caused by hurricane Bonnie (1998) for an 85 km section in the Cape Hatteras National Seashore, North Carolina. The results compare well (generally within 6%) with previous

investigations. These case studies highlight additional information gained through performing a detailed, discretized analysis using *TopCAT*.

Keywords: laser scanning, LIDAR, erosion, seacliff, topography

1. Introduction

The coastal zone is a complex, dynamic system which can experience significant morphological change, thereby affecting coastal communities, infrastructure and public resources. Understanding the processes and rates of coastal change is critical for proper management and planning. This paper presents a new Geographic Information Systems (GIS) extension, the Topographical Compartment Analysis Tool (*TopCAT*), for analyzing topographical change. The main function of *TopCAT* is to divide the study region into discrete "compartments" from which alongshore topographic and volumetric change may be quantified. This method was originally developed and demonstrated by Young and Ashford (2006b, 2007) in a manual GIS environment. *TopCAT* is designed to assist with GIS analysis of topographical data in an automated, user friendly workflow and is available for free download. *TopCAT* was specifically designed for the morphological analysis of seacliffs and beaches but may be applied to other elongated features experiencing topographical change, such as stream beds, river banks, coastal dunes, etc.

A GIS provides a powerful environment for analyzing Digital Elevation Models (DEMs), which can be created from various remote sensing techniques. This paper focuses on topographical data derived from Light Detection and Ranging (LiDAR) which pulses a high frequency laser at a target surface to obtain a swath of topographical point data. Even though some tools in *TopCAT* are specifically designed for LIDAR data, *TopCAT* is not limited to

working solely with LIDAR data and can be applied to any data that can produce continuous DEMs. Comparing sequential DEMs of an area reveals topographic change over time and provides insight into the processes and rates that drive morphological change. DEM data source and quality can have a significant influence on change detection results. For instance, Mitasova et al. (2009) examine the influence of systematic biases in airborne LiDAR data and overall impact on change analyses using DEMs. Hu et al. (2009) and Guo et al. (2010) discuss the effects of topography variability, sampling density, and interpolation method on overall DEM accuracy. Young et al. (2010) compare change detection using DEMs derived from airborne and ground-based LIDAR to evaluate seacliff erosion.

2. Background

A number of studies have explored change detection from remote sensing datasets. Coppin et al. (2004) and Lu et al. (2004) provide reviews of recent change detection algorithms. Johansen et al. (2010) discuss new post-classification comparison, image differencing, and tasseled cap transformation change detection techniques for multi-temporal imagery. In this study, LiDAR and field data provided supplemental information and validation of the imagery. Pollard et al. (2010) discusses implementation of a 3-D volumetric appearance modeling framework for change detection of areas of significant relief. This method was designed for dense urban areas, consisting of tall structures. Castilla et al. (2009) present a change detection tool focused on land cover change with applications in timber harvest monitoring. Liu et al. (2009) discuss extraction of blufflines from LIDAR data and ortho-imagery. These lines can then be used for erosion analysis. Sallenger et al. (2003) evaluated topographical change analysis of beaches using airborne LIDAR by comparison to GPS surveys. While this is only a subset of much research using LiDAR that has had significant impacts on coastal analysis, the remaining discussion will focus on tools relating to coastal change evaluation.

Some GIS tools have been previously developed to assist in the calculation of coastal change rates. Duffy and Dickson (1995) produced an ArcInfo® Macro Language (AML) program, SHOREGRID, to calculate shoreline erosion rates from digitized 2-D shorelines (from DEMs or aerial photographs, etc.) for two time intervals. The digitized shorelines are converted to grids with a value of "1" in each grid cell that would intersect the shoreline. SHOREGRID then determines the shortest distance between two shoreline grids and divides that by the time difference to determine the shoreline erosion rate. SHOREGRID also can be used to predict future shorelines based on a linear projection of the calculated erosion rates. SHOREGRID has been successfully implemented to investigate seacliff retreat (Moore et al., 1999; Moore and Griggs, 2002).

Similar to the SHOREGRID program, the Digital Shoreline Analysis System (DSAS, Thieler et al., 2008; previous version (DSMS/DSAS, Danforth and Thieler, 1992)) utilizes digitized shorelines in a GIS environment to quantify shoreline change. This tool uses regression techniques to calculate the linear change rates at specified locations between multiple digitized shorelines by casting perpendicular transects from the original shoreline. The DSAS tool has been applied successfully to evaluate seacliff top retreat (Hapke and Reid, 2007) and various beach shoreline proxies (Esteves et al., 2006; Morton et al., 2005; Harris et al., 2005; Himmelstoss et al., 2006; Pendleton et al., 2004; Hapke et al., 2010).

Although not focused on erosion, Bossak et al. (2005) developed a GIS tool, the Coastal Impact Assessment Tool (CIAT), to predict coastal storm impacts using beach slopes derived from topographic datasets, including LiDAR datasets. Additionally, the tool utilizes 3-D visualization features in GIS for scenario evaluation. The tool calculates estimated water run-ups

during storms, which provides useful information for an assessment of likely coastal damage during storm events.

The SHOREGRID and DSAS tools are primarily aimed at analyzing 2-D shoreline data; however recent advances in coastal remote sensing now provide high-resolution, 3-D topographical data. The *TopCAT* GIS extension was developed to build upon the SHOREGRID and DSAS tools to incorporate the use of a 3-D environment. Working with *TopCAT* and 3-D data provides several advantages compared to 2-D data. First, *TopCAT* is not limited to transects, but instead works with the entire data grid thereby accounting for the data between transects. Second, *TopCAT* can account for bends in the shoreline; transects at close intervals can overlap in these locations, forcing a larger sampling interval, which could limit the ability of the user to study localized phenomena. Next, a vectorized approach requires the user to select the top, base, or other consistent location of the cliff for comparative analysis. Young et al. (2009a) discuss how estimates of cliff retreat vary depending on whether the cliff top, base, or face is used for comparison. *TopCAT,* in contrast, uses 3-D data of the entire cliff face to estimate mean cliff face retreat. Finally, *TopCAT* allows for continuous volumetric analysis which provides valuable information for sediment budget analysis.

A limitation worth noting is that because high resolution topographic datasets have only become recently available, *TopCAT* may not be applicable to historical shoreline analysis which relies on 2-D data sets. Further, DSAS uses weighted regression analysis for multiple time series shore-lines, where-as *TopCAT* is currently designed to work with only two datasets at a time. Because *TopCAT* operates within *ArcGIS* and implements spatial analyst tools, it inherits many processing limitations (e.g. size of dataset) that the user would experience in *ArcGIS*

implementing those tools manually. Generally, this is most significant when generating DEM datasets for sections of large (> 50 km) extents with small cell sizes (<1m).

Portions of *TopCAT* and the general topographic change compartment methodology have been successfully implemented in several recent coastal cliff coastal geomorphic studies in Southern California (e.g. Young et al., 2009a; 2009b; 2010; 2011). This paper will show two additional case studies to highlight how tools from TopCAT can be helpful for such studies.

3. Methodology

3.1 Procedure

The *TopCAT* program (Figure 1) runs through Visual Basic for Application (VBA) routines created within ArcView® GIS 9.x and 10.x Software (ESRI, 2005). Prior to using *TopCAT*, the user creates ESRI DEM grid files of two sequential topographical datasets for the area of interest. Once the user has created the DEM grids, *TopCAT* routines can be easily and quickly implemented with the following steps (1-5) for beach studies and a few additional steps (6-7) for seacliff erosion studies or other optional analyses (8 and 9):

1. Create a volume change grid by differencing two digital elevation models using the *Elevation Change Grid Creation Tool.* This tool also allows the user to create a grid with net, positive only, or negative only change.
2. Define boundaries to remove unwanted or erroneous data (i.e. vegetation, waves, data outside the boundary of interest, etc). Polygons can be digitized around these areas that show irregularities (e.g. vegetation, waves) and a supplementary grid clipper tool from *TopCAT* can be used to remove those sections from the grid.
3. Draw a centerline through the data to show the general alongshore trend of the coastline. This can be automated through the *Centerline Creation Tool*.

4. Run the *Compartment Creation Tool* () to create distinct compartments along the centerline.
5. Calculate the volume differences of cells within each compartment using the *Compartment Analysis Tool.*
6. Run the *Height Finder Tool* to obtain cliff heights (seacliff analysis only).
7. Calculate the average cliff face retreat/advance rate using the *Retreat Rate Calculator Tool* (seacliff analysis only).
8. Optional: Implement the *Sediment Budget Analysis Tool* (sea cliff analysis only).
9. Optional: Draw polylines intersecting compartments along the shoreline to delineate regions of different categories. Use the *Categorization Tool* to assign a category label to each compartment.

From the output results of *TopCAT,* the user can then plot the data and perform statistical analyses using the results for the individual compartments or perform further comparisons.

3.2 Additional tools

TopCAT provides other useful tools to increase productivity in GIS while working with DEMs and LIDAR data, including:

- *Subdivide Compartments Tool* – If the user decides that they want to perform a finer-scale analysis, this tool subdivides larger compartments into smaller compartments.
- *Profile Tool* - Creates profiles of DEMs perpendicular to centerline spaced at any of the following: transects spaced at equal intervals along a polyline, through the center of each compartment, or through designated polylines drawn by the user along a section of interest.

- *Point cloud data coloring tool* – Applies color from ortho-imagery to point cloud datasets. For example, many airborne LiDAR datasets do not have RGB color values associated with them. This tool enables the user to color the point cloud, as shown in Figure 3. Note that the best results are achieved when limited time has elapsed between acquisition of the LiDAR data and image and under the same conditions (e.g. low tide).
- *Root Mean Square (RMS) Calculator* - Calculates the RMS differences in elevation values between two grids and can be used in one of two ways. First, it can be used for error assessment when both grids contain only unchanged areas. For example, an unchanging surface such as a roadway can be used to evaluate biases between datasets (Mitasova, 2009). Second, it can be used to quickly assess the general amount of change between two datasets when implemented for the entire area of interest.
- *Grid Clipper Tool* – Clips a grid extents based on a polygon. This tool can be used for extracting roadways and other unchanging sections for RMS calculations, removing vegetation or water from the DEM, or limiting the area of analysis.
- *Pulse Extractor Tool* - Extracts a specific LIDAR return pulse from a ASCII text file with multiple returns.
- *Grid Converter Tool* - Converts a floating point ASCII grid into an ESRI grid. Currently, *ArcGIS* only imports ASCII grids with integer values.

3.3.Mechanics

As previously mentioned, the *TopCAT* program was designed to automate the procedure described in Young and Ashford (2006b) for topographical change analysis of seacliffs. This method divides the coastline into compartments using a centerline as a guide (Figure 2). These compartments enable both statistical and discretized analysis. Typically, the user would digitize

188 a simplified centerline as a polyline along the section of interest, capturing the curves most
189 important for their analysis. The ideal centerline would parallel the coastline and be, more or
190 less, equidistant from the seaward and landward edges of the datasets. To produce the best
191 results in creating the compartments and minimize digitization time, the centerline should be
192 simple, avoiding jagged edges and sharp turns. The centerline would be similar to a shoreline
193 digitization; however, the user should only follow major curves and trends along the coastline
194 and does not need to digitize small curves. The C*enterline Creation Tool* automates the
195 procedure by tracing the contour the average cliff height elevation, as determined from a DEM,
196 but generally requires some simplification for compartment creation.

197 After a centerline is created, the user runs the *Compartment Creation* Tool. The basic
198 inputs to this routine are the desired compartment width, (*w*) and the offset distance (*l*) (Figure
199 2). To construct these compartments, the routine creates a copy of the centerline on the left and
200 on the right of the centerline by the specified offset distance. The routine then marches along the
201 centerline by subdividing the centerline to the specified compartment width and finds the nearest
202 points on the lines copied on the left and the right for the subdivision's start and end nodes.
203 These four new points along with the line segments between these points are used to create a
204 polygon compartment whose area is checked to ensure equal area compartments (within a typical
205 tolerance of 1%), which is particularly important at rounded corners where the compartments
206 must fan around a vertex (Figure 2). If the compartment area is within the tolerance, the routine
207 moves on to the next segment and repeats the process. If the area is not within the tolerance,
208 then the routine will iteratively increase or decrease the centerline segment size by a small
209 amount until the compartment area complies. Both the area and width of the compartment are
210 stored in the shapefile for future reference. If it is more important that the compartments have

211 equal width rather than area (e.g. when the change grid does not span the entire width of the
212 compartments), then the user can relax the area tolerance to preserve equal width along the
213 centerline.

214 In areas where the coastline may have sharp corners and bends, *TopCAT* has custom
215 options to find and smooth these sections of the centerline. The smooth line option in *ArcGIS*®
216 can be performed as part of the routine, thus the user does not need to manually run this
217 processing step separately. If a large offset distance is used, the centerline can be densified to
218 use more vertices thereby producing smoother curves. This option may be necessary because
219 *ArcGIS*® uses a series of lines with vertices to approximate curves. In addition, an advanced
220 option can be enabled to find areas where there is a sharp corner and fan the compartments as
221 triangles around that point rather than have a sharp kink in the middle of the compartment
222 (Figure 2). The compartment creation routine was designed to avoid as much interaction as
223 possible in the creation of the compartments and in general, these advanced options are not
224 necessary. However, after the compartments are created, the user can make manual edits or
225 change the parameters to recreate the compartments if desired.

226 Following the compartment creation, the user runs the *Compartment Analysis Tool* which
227 utilizes the *ArcGIS*® Zonal Statistics functions in the Spatial Analyst extension to determine
228 volume change statistics from the elevation change grid such as the sum, average, range,
229 maximum and minimum volume change per cell within each compartment. The total
230 compartment volume change is calculated by:

231

232 $$\boldsymbol{E = A_{cell} \times \sum_{i=0}^{i=n_{cell}} dz_i}$$ Equation 1

233

where:

E = the eroded compartment volume, m^3,

A_{cell} = the area of a grid cell, m^2,

n_{cell} = the number of cells in the compartment, and

d_{zi} = the value of elevation difference, m, of the i^{th} cell in the compartment from the elevation change grid.

These values are then normalized by the width of the compartment to get the alongshore volumetric change per unit width. With this data available, localized scale change analysis can be performed.

Following the volumetric analysis, two additional steps are required for a seacliff analysis that are not run for a beach or coastal dune change analysis. By running the *Height Finder Tool*, the user can assign a seacliff height to each compartment. The routine finds the highest value on a DEM within each compartment to represent the seacliff height. Alternatively, in developed areas where buildings, trees, etc. are on top of the seacliff and would be the highest value on the DEM for the compartment, the user can use a digitized polyline representing the top of the seacliff to guide the assignment of a proper seacliff height from the DEM. Once height values are obtained, the user then runs the *Retreat Rate Calculation Tool* which calculates the average cliff face retreat rate (Figure 4, modified from Young and Ashford 2006a) from:

$$\boldsymbol{R = E/(h * w * t)} \quad \text{Equation 2}$$

where:

R = the average cliff face retreat rate (m/year)

257 E = the eroded compartment volume (m^3), calculated in Equation 1,

258 h = the height of the cliff in the compartment (m),

259 w = the compartment width along the centerline (m), and

260 t = the time difference between the datasets (yr).

261 In regions where seacliffs provide sediment to the littoral system, *TopCAT* can calculate
262 coarse sediment yield. Coarse grained sediment (diameter larger than the littoral cutoff diameter,
263 LCD) contributes to the sediment to the littoral system (Hicks, 1985) while finer sediment
264 (diameter less than the LCD) will not remain on the beach. The percentage of coarse material
265 within the seacliffs may be evaluated using the littoral cutoff diameter (Hicks, 1985) and sieve
266 analysis. A percentage of coarse material can be used for cliff coarse-sediment yield analyses
267 using *TopCAT* through one of three methods, depending on the amount of information available
268 and the extents of the area analyzed. First, the user can assign a constant value to the entire
269 region if limited information is available. Second, the user can digitize polylines to delineate
270 areas with similar percentages of coarse material, which are assigned to the compartments by
271 intersecting the polyline. Third, the user may manually enter a percentage for each compartment
272 if detailed data are available.

273 The seacliff coarse sediment yield is then determined by reducing the total eroded
274 volume to the percentage of coarse material within the cliff-forming material (Equation 3). The
275 routine calculates the annual seacliff coarse sediment yield using the equation:

276

277 $$Q_S = \sum_i Q_i \times \%coarse_i \,/\, t \qquad \text{Equation 3}$$

278

279 Where:

280 Q_S = the rate of seacliff coarse sediment yield (m^3/year),

281 E_i = the total volume change for the seacliffs (m^3) in compartment *i*,

282 $\%coarse_i$ = the percent of coarse sediment in the seacliffs in a compartment *i*, and

283 *t* = time period (years)

284 *3.4 Categorization Analysis*

285 Change rates often are dependent on many variables such as soil types, groundwater
286 conditions, erosion control, development, etc. To compare the effects of these variables, a
287 *TopCAT* tool was developed to automate compartment categorization and then determine the
288 influence of those variables on topographic change. In this procedure the user creates digitized
289 polylines (Figure 2) delineating the different features and assigns categories to each polyline. If
290 a polyline intersects a compartment, the routine assigns the corresponding category to the
291 compartment. In the example illustrated in Figure 2 where polylines delineate erosion control,
292 compartments 1-7 would be classified as rip-rap, 8-11 would be classified as un-protected, and
293 12-16 would be classified as a concrete sea wall. The tool outputs a table showing the
294 compartmental change for each category and the percent contribution of that category to the
295 overall change to evaluate effectiveness using the following equation (Young and Ashford
296 2006b):

297

298 $$PE = [(R_U - R_V)/R_U] \times 100\% \qquad \text{Equation 4}$$

299

300 where:

301 *PE* = Percent Effectiveness,

302 R_U = the rate for the unclassified (natural) portions, and

303 R_V = the rate for the specific variable, *V*, (i.e. type of protection for this example).

304 To implement this comparison using the *Categorization Analysis Tool*, the user delineates
305 polylines representing areas protected by each type of structure and assigns a category identifier
306 for each type. The *TopCAT* routine then determines what type of erosion control is present in
307 each of the compartments, if any, and evaluates the overall effectiveness of each type by a
308 comparison with unprotected compartments.

309 *3.5 Error Assessment*

310 The *RMS Calculation Tool* can be used for an error assessment. To implement this tool,
311 one should generate clipped version of each temporal grid (e.g. using the *Grid Clipper Tool*) so
312 that only features expected to remain fixed during the time of the study remain. These features
313 could be roads, rooftops, parking lots, concrete structures, etc. If none such features are available
314 in the dataset, one could estimate the RMS at areas that show no-minimal change (e.g. hard rock
315 far from the water). However, the latter approach should be implemented with extreme caution
316 because this could (1) overestimate the error because it would interpret change as error, or (2)
317 underestimate the error because of a systematic error in one dataset more or less cancels out with
318 the amount of change that occurred between the datasets.

319 ***4. Case Study Results and Discussion***

320 *4.1 Case Study I – Dog Beach, Del Mar, CA*

321 To demonstrate the applicability of *TopCAT* to seacliff erosion analysis, *TopCAT* was
322 used to evaluate a 500 m segment in Del Mar, California (Figure 5). Topographic data collected
323 from terrestrial LIDAR surveys in October 2005 and March 2007 were gridded into DEMs at 0.5
324 m resolution using IDW interpolation. Olsen et al. (2009 and 2011) describes the techniques
325 used to collect and geo-reference these datasets. The vertical RMS error between the DEM

326 datasets was evaluated by comparing the elevation differences between the two DEMs on a
327 control surface (a concrete covered slope (approximately 600 m^2) immediately north of the study
328 area) and was found to be 0.13 m using the *RMS Calculation Tool*. Note that the RMS between
329 points in the two point cloud datasets was calculated to be 0.05 m. Hence, the process of
330 gridding using IDW in the XY horizontal plane introduced some additional error, particularly
331 given the steep slope of the cliffs.

332 *TopCAT* was then implemented with a 2 m compartment width to evaluate the alongshore
333 (Figure 6) and overall morphology (Table 1). The results for the entire section (Table 1) show an
334 average cliff face retreat rate of 4.9 cm/year and an average loss of 1 m^3 /m-yr. The total
335 volume of sediment loss for the study area during the 1.5 year period was 745 m^3 (~500 m^3/yr.)

336 The calculated volumes for failure sites F1, F2, and F3 using *TopCAT* showed consistent
337 results (<10% difference, Table 2) to volumes calculated using 3-D TIN surfacing methods
338 available in commercial software. Cliff retreat rates obtained through *TopCAT* are generally
339 consistent with previous studies (e.g. Everts, 1991; Benumof et al., 2000; Young and Ashford,
340 2006a; Hapke and Reid, 2007; Young et al, 2009b), which estimate mean cliff retreat rates at or
341 near the studied cliff section between 4-20 cm/yr. Note that while the 4.9 cm/year obtained
342 using *TopCAT* is at the lower end of this range of values, the datasets used in this study were of a
343 relatively short (1.5 year) period, which was relatively dry.

344 Performing a regional analysis for this study area could lead to the conclusion that
345 seacliff retreat occurs relatively slowly (average of 4.9 cm/year during the study period).
346 However, *TopCAT* reveals that the erosion was dominated by two large (>250m^3) failure events
347 (F1& F2 in Figure 6) which accounted for over 80% of the volume change for the study area.
348 Figure 7 shows a typical cross section at Site F1. Figure 6 shows localized retreat rates as high

as 1.4 m/year, indicating the average does not provide a complete understanding of the erosional patterns. Thus, finer scale analysis available with *TopCAT* provides insight on the variable and episodic nature of seacliff retreat and can be used to highlight and isolate areas of interest to improve understanding of geologic processes along subsections of coast. However, further evaluation of using a long-term dataset will be important to determine the overall contribution of large versus smaller erosion events to the overall sediment loss from the cliffs.

4.2 Case Study II – North Cape Hatteras National Seashore, North Carolina

To demonstrate the application of *TopCAT* to volumetric beach and dune change, *TopCAT* was applied to an 85 km segment of Cape Hatteras National Seashore in North Carolina (Figure 8) immediately south of the Oregon Inlet. Meridith et al. (1999) previously studied the Cape Hatteras National Seashore as part of an analysis of volumetric change of beach sand on the east coast following Hurricane Bonnie. For that study, sections approximately 22 km in length were used. The results of that previous study will be used to validate the *TopCAT* tool and show some features that *TopCAT* offers to enhance such studies.

Airborne LIDAR datasets of the region from Fall 1997 and Fall 1998 (post Hurricane Bonnie) were obtained through NOAA Digital Coast (2010) to analyze the volumetric change induced by Hurricane Bonnie (August 19-30, 1998). Ideally, the before dataset would be collected immediately prior to the Hurricane for hurricane related damage assessment. However, the focus of this paper is to demonstrate the tools of *TopCAT*. These datasets were estimated to have a vertical accuracy of 0.15 m (NOAA, 2010). DEMs with a cell size of 5 m were created using the mean elevation of all LiDAR points within each grid cell (Olsen 2011).

The RMS tool in *TopCAT* calculated a RMS of 0.21 m between the DEMs created from the 1997 and 1998 datasets for a 10 km section of the highway, whose boundaries were roadway were digitized using available ortho-imagery combined with the LiDAR DEM. For validation,

zonal statistic functions in the Spatial Analyst toolbar in *ArcGIS* calculated a mean difference of -0.111 m and standard deviation of 0.176 m for the roadway. Using the statistical relationship $RMS^2 = mean^2 + std\ dev.^2$, produces a RMS value of 0.208 m, in agreement with *TopCAT*. A recent study by Mitasova et al. (2009) evaluated errors of airborne LiDAR datasets in this area by comparing the LiDAR data to RTK GPS coordinates. Although a direct comparison was not available in that study, the results are consistent with the range of values observed between airborne LiDAR datasets in the area.

Boundaries for the change analysis (Figure 9) were designated as the water's edge for the seaward side and vegetation, structures, or roadways to delineate for the landward boundary. Boundaries were digitized to be consistent with Meredith et al. (1999) interpretation shown in several figures in that report. Because the primary purpose of the analysis herein is to evaluate the effectiveness of the tool rather than perform a scientific analysis, the datasets were not adjusted for bias between surveys (as recommended by Mitasova et al. (2009)) to remain consistent with Merdith et al. (1999). However, bias adjustments should be applied prior to using *TopCAT* for scientific analyses.

Figure 10 shows the compartmentalization along Cape Hatteras using 100 m wide compartments. Because of the complex nature of the cape, a minimal amount of manual editing following the automatic compartment creation was required to extend the compartments to cover the entire cape. In most cases, manual editing is not required. Volumetric change per unit length of coastline highlights *TopCAT*'s ability to provide alongshore variability at fine intervals. Table 3 summarizes overall change statistics for the entire section. Note that the maximum accretion (582 m^3) occurred on the cape itself. The alongshore calculations from *TopCAT* (e.g. Figure 10) provide a more detailed picture of the erosion-accretion relationship compared to the general

summary statistics. Figure 11 shows a cross section (generated using the *Profile Tool*) near the cape, highlighting the extent of erosion of the dunes and minimal accretion behind the original dune.

The results from *TopCAT* were verified against raster statistics calculated in GIS to ensure computational integrity. The results computed for overall change also compare well (Table 3) with those of Meridith et al. (1999). Potential reasons for the differences in values between the studies include (1) differences in interpretation for boundary digitization, and (2) different interpolation techniques for DEM creation (Meredith et al. 1999 used inverse distance weighted interpolation compared to the mean cell value used for this study).

5. Conclusions

This paper presents a new GIS based tool (*TopCAT*) which provides a user-friendly interface for automated volumetric change analysis of large topographical datasets along with several tools to enhance DEM and LIDAR data processing. The tool was developed to provide high resolution visual and statistical morphological change metrics using a discrete compartmentalization method. Performing change analysis in *TopCAT* provides large-extent regional analysis, but, in addition, *TopCAT* provides the ability to hone in on smaller subsections of an area where localized events can be further analyzed. Detailed results from *TopCAT* reveals erosional hot spots and alongshore coastal change trends not readily visible when performing overall and average change detection for a region. These details provide additional insight of potential hazards or existing damage which can be underestimated in a large extent analysis. While *TopCAT* was applied to examples presented in this paper for seacliff and beach topographic analysis, *TopCAT* can be a beneficial tool for similar elongated features that

418 experience topographical change. *TopCAT* is publically available for free download at
419 (http://engr.orst.edu/~olsen/software/*TopCAT*/).

420 ***Acknowledgements***

421 The authors would like to thank Elizabeth Johnstone and Jessica Raymond for performing
422 LIDAR survey work in Del Mar, CA. Maptek I-Site provided software used for the analysis and
423 manipulation of the LiDAR data. NOAA Digital Coast provided airborne LiDAR datasets. This
424 research was partially funded via a grant from California Seagrant (Project #R/OE-39), the
425 Coastal Environmental Quality Initiative (CEQI) under award #04-T-CEQI-06-0046, and the
426 University of California, San Diego Chancellor's Interdisciplinary Collaboratories Fund. The
427 above support is greatly appreciated. We also appreciate the valuable comments provided by the
428 anonymous reviewers of this article.

429 ***References***

430 Bossak, B.H., Morton, R.A., Sallenger, A.H., 2005. A GIS-based information system for
431 predicting impacts from coastal storms – the Coastal Impact Assessment Tool (CIAT),
432 Version 1.0, User's Manual, U.S. Geological Survey Open-File Report 2005-1260, 28 pp.,
433 URL: http://pubs.usgs.gov/of/2005/1260/ (accessed 29 July 2011).

434 Benumof, B.T., G.B. Griggs, 1999. The Dependence of Seacliff Erosion Rates on Cliff Material
435 Properties and Physical Processes: San Diego County, California, Shore & Beach 67(4), 29-
436 41.

437 Benumof, B.T., Storlazzi, C.D., Seymour, R.J., Griggs, G.B., 2000. The relationship between
438 incident wave energy and seacliff erosion rates: San Diego County, California, Journal of
439 Coastal Research, 16(4), 1162–1178.

440 Castilla, G., Gurthrie, R.H., Hay, G.J., 2009. The Land-cover change mapper (LCM) and its

441 application to timber harvest monitoring in western Canada, Journal of Photogrammetric
442 Engineering and Remote Sensing, 75(8), 941-950.
443 Coppin, P., Jonckheere, I., Nackaerts, K., Muys, B., Lambin, E., 2004. Digital change detection
444 methods in ecosystem monitoring: A review, International Journal of Remote Sensing, 25(9),
445 1565-1596.
446 Danforth, W.W., Thieler, E.R., 1992. Digital Shoreline Analysis System (DSAS) User's Guide,
447 Version 1.0, US Geological Survey Open-File Report 92-355, 42pp.
448 Duffy, W., Dickson, S.M., 1995. Using Grid and Graph to Quantify and Display Shoreline
449 Change, Proceedings 1995 ESRI International User Conference, pp. 74.
450 Esteves, L.S., Williams J.J., Dillenburg, S.R., 2006. Seasonal and interannual influences on the
451 patterns of shoreline changes in Rio Grande do Sul, southern Brazil, Journal of Coastal
452 Research, 22(5), 1076–1093.
453 Everts, C.H., 1991. Seacliff retreat and coarse sediment yields in southern California,
454 Proceedings Quantitative Approaches to Coastal Sediment Processes, Seattle, Washington,
455 1586–1598.
456 Guo, Q., Li, W., Yu, H., Alavrez, O., 2010. Effects of topographic variability and LIDAR
457 sampling density on several DEM interpolation methods, Journal of Photogrammetric
458 Engineering and Remote Sensing, 76(6), 701-712.
459 Harris, M., Brock, J., Nayegandhi, A., Duffy, M., 2005. Extracting shorelines from NASA
460 airborne topographic Lidar-derived digital elevation models, US Geological Survey Open
461 File Report 2005-1427, 39 pp, URL: http://pubs.usgs.gov/of/2005/1427/ofr-2005-1427.pdf
462 (accessed 29 July 2011).
463 Hapke, C., Richmond, B., 2000. Monitoring beach morphology changes using small-format

464 aerial photography and digital softcopy photogrammetry, Environmental Geosciences,
465 Special Issue on Coastal Hazard Mapping Techniques, 7, 32-37.
466 Hapke, C.J. Reid D., 2007. National Assessment of Shoreline Change Part 4: Historical Coastal
467 Cliff Retreat along the California Coast, US Geological Survey Open File Report 2007-1133,
468 57 pp., URL: http://pubs.usgs.gov/of/2007/1133/of2007-1133.pdf (accessed 29 July 2011).
469 Hapke, C.J., Himmelstoss, E.A., Kratzmann, M., List, J.H., and Thieler, E.R., 2010, National
470 assessment of shoreline change; historical shoreline change along the New England and Mid-
471 Atlantic coasts: U.S. Geological Survey Open-File Report 2010-1118, 57 pp., URL:
472 http://pubs.usgs.gov/of/2010/1118/ (accessed 29 July 2011)
473 Hicks, D. M., 1985. Sand dispersion from an ephemeral delta on a wave-dominated coast, Ph.D.
474 dissertation, Earth Sciences Dept., University of California, Santa Cruz, 210pp.
475 Himmelstoss, E.A.; Fitzgerald, D.M.; Rosen, P.S., Allen, J.R., 2006. Bluff evolution along
476 coastal drumlins: Boston Harbor Islands, Massachusetts, Journal of Coastal Research, 22(5),
477 1230–1240.
478 Hu, P., Liu, X., Hu, H., 2009. Accuracy assessment of Digital Elevation Models based on
479 approximation theory, Journal of Photogrammetric Engineering and Remote Sensing, 75(1),
480 49-56.
481 Johansen, K., Arroyo, L.A., Phinn, S., Witte, C., 2010. Comparison of Geo-Object-Based and
482 Pixel-Based Change Detection of Riparian Environments using High Spatial Resolution
483 Multi-Spectral Imagery, Journal of Photogrammetric Engineering and Remote Sensing,
484 76(2), 123-126.
485 Liu, J.K., Li, R., Deshpande, S., Niu, X., Shih, T.Y., 2009. Estimation of blufflines using
486 topographic lidar data and orthoimages, Journal of Photogrammetric Engineering and

Remote Sensing, 75(1), 69-79.

Lu, D., Mausel, P., Brondizon, E., Moran, E., 2004. Change detection techniques, International Journal of Remote Sensing, 25(12), 2365-2407.

Meridith, A., Eslinger, D., Aurin, D., 1999. An evaluation of hurricane-induced erosion along the North Carolina Coast using airborne LIDAR surveys, CSC Technical Report NOAA/CSC/99031-PUB, 35pp., URL: ftp://www.csc.noaa.gov/pub/crs/reports/bonnie/BonnieTechReport.pdf (accessed 29 July 2011).

Mitasova, H., Overton, M.F., Recalde, J.J., Bernstein, D.J., Freeman, C.W., 2009. Raster-based analysis of coastal terrain dynamics from multitemporal lidar data, Journal of Coastal Research 25(2), 507-514.

Moore, L.J., Benumof, B., Griggs, G.B., 1999. Coastal erosion hazards in Santa Cruz and San Diego Counties, California, Journal of Coastal Research, SI(28), 121-139.

Moore, L.J., Griggs, G.B., 2002. Long-term cliff retreat and erosion hotspots along the central shores of the Monterey Bay National Marine Sanctuary, Marine Geology, 181(1-3), 265-283.

Morton, R.A., Miller, T., Moore, L., 2005. Historical shoreline changes along the US Gulf of Mexico: A summary of recent shoreline comparisons and analyses, Journal of Coastal Research, 21(4), 704–709.

NOAA (2010). Digital Coast – NOAA Coastal Services Center, URL: http://www.csc.noaa.gov/digitalcoast/NOAA, (accessed 05 July 2010).

Olsen, M.J., (2011). Bin 'N' Grid: A simple program for statistical filtering of point cloud data, *LIDAR news* 1(10), URL: http://www.lidarnews.com/content/view/8378/136/, (accessed 1 October, 2011).

Olsen, M.J., Johnstone, E., Kuester, F., Ashford, S.A., Driscoll, N., 2011. New automated point-

510 cloud alignment for ground based LIDAR data of long coastal sections, Journal of Surveying
511 Engineering, 137(1), 14-25.
512 Olsen, M.J., Johnstone, E., Driscoll, N., Ashford, S.A., Kuester, F., 2009. Terrestrial laser
513 scanning of extended cliff sections in dynamic environments: a parameter analysis," Journal
514 of Surveying Engineering, 135(4), 161-169.
515 Pendleton, E.A., Williams, S.J., Thieler, E.R., 2004. Coastal vulnerability assessment of
516 Assateague Island National Seashore (ASIS) to sea-level rise, U.S. Geological Survey Open-
517 File Report 2004-1020, 20 pp., URL: http://pubs.usgs.gov/of/2004/1020/ (accessed 29 July
518 2011).
519 Pollard, T.B., Eden, I., Mundy, J.L., Cooper, D.B., (2010). A Volumetric Approach to Change
520 Detection in Satellite Images, Journal of Photogrammetric Engineering and Remote Sensing,
521 76(7), 817-831.
522 Sallenger, A.H, Krabill, W.B., Swift, R.N., Brock.J, List, J., Hansen, M., Holman, R.A.,
523 Manizade, S., Sontag, J., Meredith, A., Morgan, K., Yunkel, J.K., Frederick, E.B., Stockdon,
524 H., 2003. Evaluation of airborne topographic LIDAR for quantifying beach changes,
525 Journal of Coastal Research, 19(1), 125-133.
526 Thieler, E.R., Himmelstoss, E.A., Zichichi, J.L., Ergul, A., 2008. Digital Shoreline Analysis
527 System (DSAS) version 4.0—An *ArcGIS* extension for calculating shoreline change, U.S.
528 Geological Survey Open-File Report 2008-1278, URL: http://woodshole.er.usgs.gov/project-
529 pages/dsas/version4/ (accessed 29 July 2011)
530 Young, A.P., Ashford, S.A., 2006a. Application of airborne LIDAR for seacliff volumetric
531 change and beach sediment budget contributions, Journal of Coastal Research, 22(2), 307-
532 318.

533 Young, A.P., Ashford, S.A., 2006b. Performance Evaluation of Seacliff Erosion Control
534 Methods, Shore and Beach, 74(4), 16-24.
535 Young, A.P., Ashford, S.A. 2007. Quantifying sub-regional seacliff erosion using mobile
536 terrestrial LIDAR, Shore and Beach, 75(3), 38-43.
537 Young, A.P., Flick, R.E., Gutierrez, R., Guza, R.T., 2009a. Comparison of short-term seacliff
538 retreat measurement methods in Del Mar, California, Geomorphology, 112(3-4), 318-323.
539 Young, A.P., Guza, R.T., Flick, R.E., O'Reilly, W.C., Gutierrez, R., 2009b. Rain, waves and
540 short-term evolution of composite seacliffs in southern California, Marine Geology, 267(1-
541 2), 1-7.
542 Young, A.P., Olsen, M.J., Driscoll, N., Gutierrez, R., Guza, R.T., Flick, R.E., Johnstone, E.,
543 Kuester, F., 2010. Mapping Seacliff Erosion with Terrestrial and Airborne LIDAR, Journal
544 of Photogrammetric Engineering and Remote Sensing, 76(4), 421-427.
545 Young, A.P., Guza, R.T., O'Reilly, W.C., Flick, R.E., Gutierrez, R., 2011. Short-term retreat
546 statistics of a slowly eroding coastal cliff, Natural Hazards and Earth Systems Sciences,
547 11(1), 205-217.
548

549 **Table 1 - Compartamental statistics using *TopCAT* for Dog Beach, Del Mar California (Oct**

550 **2005- March 2007)**

Statistic	Average cliff face Retreat rates (cm/year)	Volume per Unit length per year (m^3/m-yr)
Average	**-4.90**	**-1.0**
Max Erosion	**-144**	**-32.7**
Max Accretion	13.9	3.4
Std Dev	17.7	3.8

551

552

553 **Table 2. Comparisons of erosional volumes using 3-D volumetric analysis and *TopCAT***

554 **compartmental analysis.**

555

Failure site	TIN 3-D Vol (m^3)	*TopCAT* Vol (m^3)	% Difference
F1	263	251	-4.6%
F2	312	346	11.1%
F3	42	46	10.0%
Sum	**617**	**644**	**4.3%**

556

557

558

559

560

561

562

563

564 **Table 3. Comparisons of erosional volumes calculated using *TopCAT's* compartmental**

565 **analysis to results from Merdith et al. (1999).**

566

Analysis Variable	Merdith et al. (1999)	*TopCAT*	% Difference
Average net sand loss/length	-41.0 m^3/m	-38.8 m^3/m	-5.3%
Average net sand loss/area	-0.37 m^3/m^2	-0.47 m^3/m^2	25.4%
Net volume loss	-3,517,000 m^3	-3,362,960 m^3	-4.4%
Volume loss (cut)	-4,205,000 m^3	-4,009,722 m^3	-4.6%
Volume gain (fill)	688,000 m^3	646,762	6.0%
Compartment Analysis			
Max sand loss/length	N/A	-168 m^3/m	N/A
Max sand accretion/length	N/A	582 m^3/m	N/A
Hotspot Evaluation			
Maximum vertical loss	>6m	7.4m	N/A

567

Figures

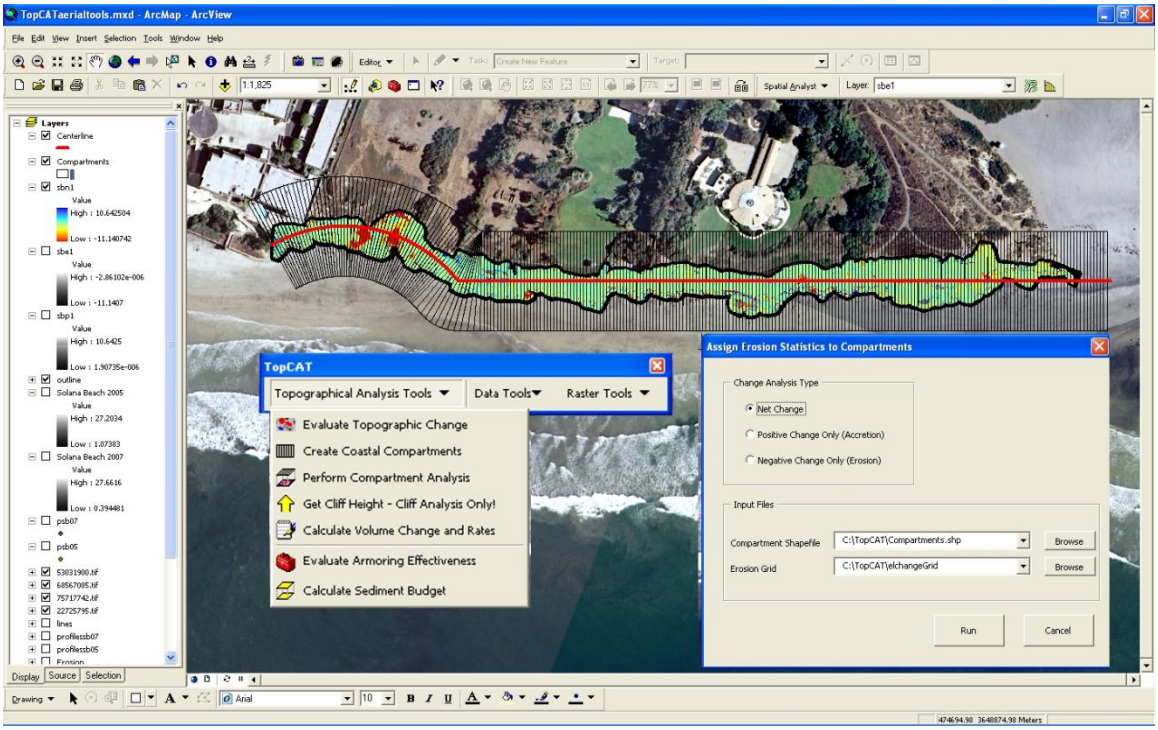

Figure 1 - *TopCAT* toolbar and user interface in ESRI *ArcGIS*®. The centerline used to generate the compartments is shown in red, the compartments are shown in black. The erosion change grid is overlain on the aerial photography.

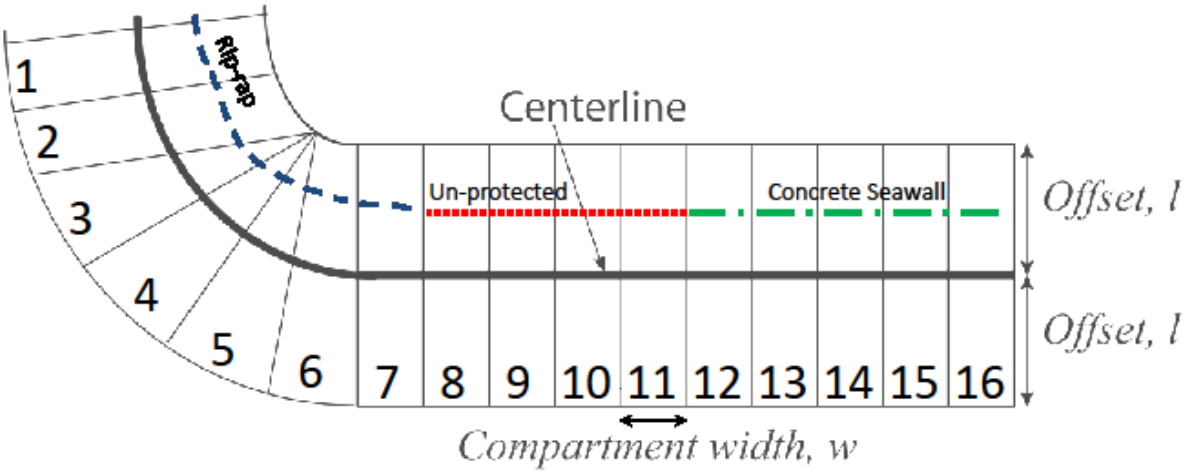

577

578

579 **Figure 2 – Schematic for compartment creation using a centerline as a guide. The dashed**

580 **and dotted lines represented digitized polylines representing various erosion control**

581 **devices. These polylines can be used to categorize each compartment based on shoreline**

582 **protection, which enables users to compare the effectiveness of these protection techniques.**

583

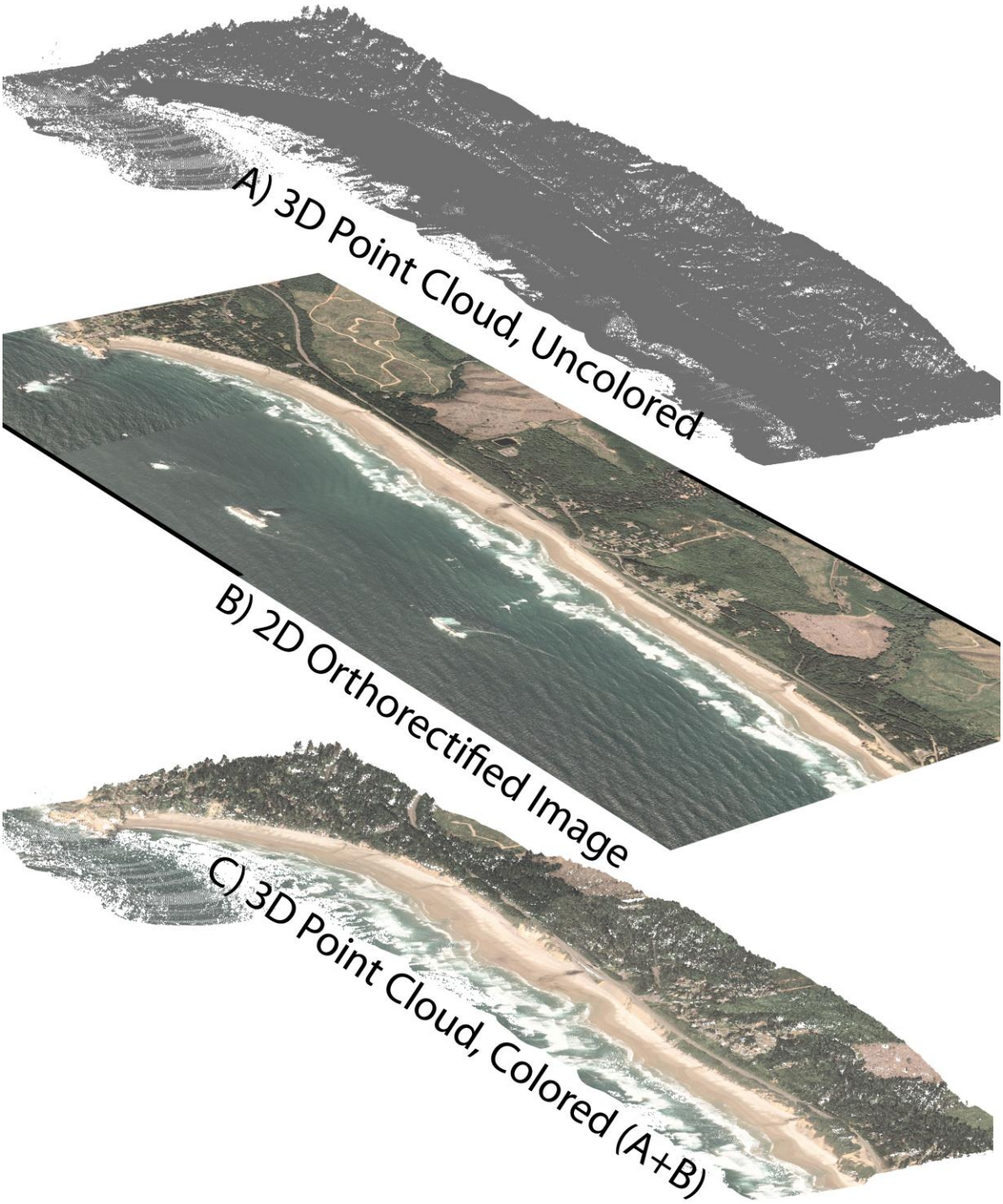

Figure 3 – Illustration of the procedure for colorization of a point cloud of the Oregon Coast from an ortho-rectified photograph. The point cloud was obtained through NOAA Digital Coast and the image was obtained through the USGS and were not acquired at the same time.

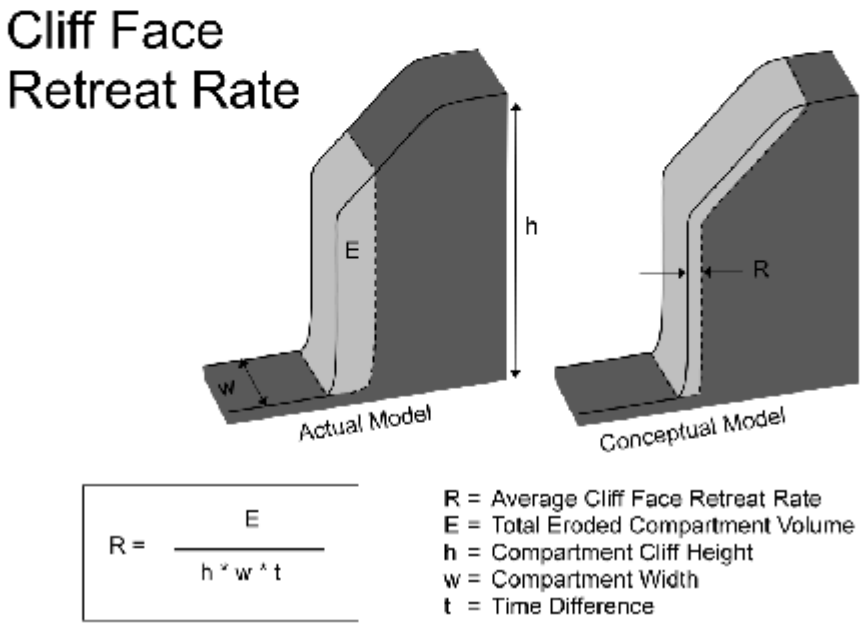

589
590 **Figure 4 - Geometric relationship between the average seacliff face retreat and the**
591 **calculated compartment seacliff change volume (modified from Young and Ashford,**
592 **2006a).**

593

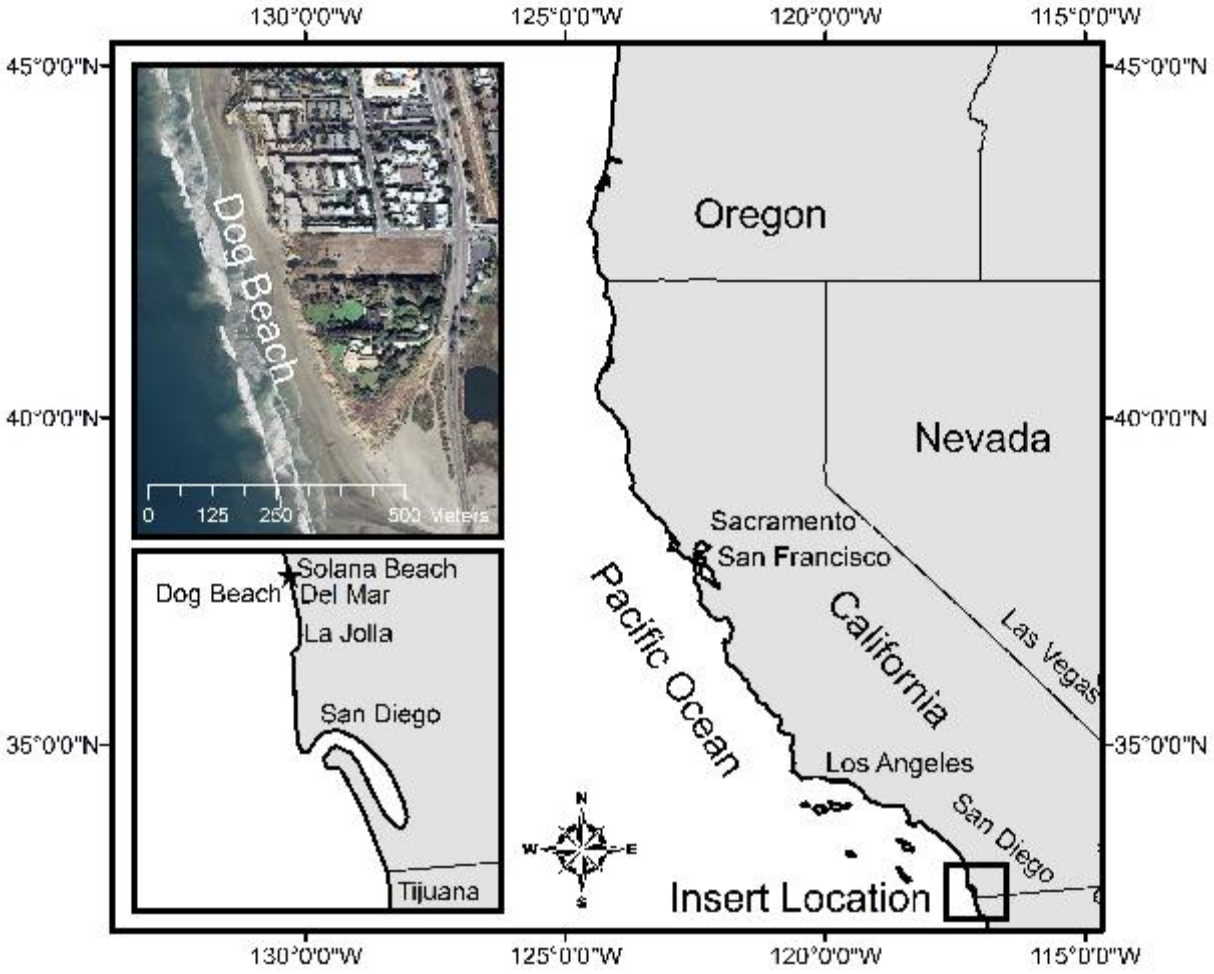

595
596 **Figure 5 – Map showing the location and aerial photography the site for Case Study #1 in**

597 **Del Mar, California.**

598

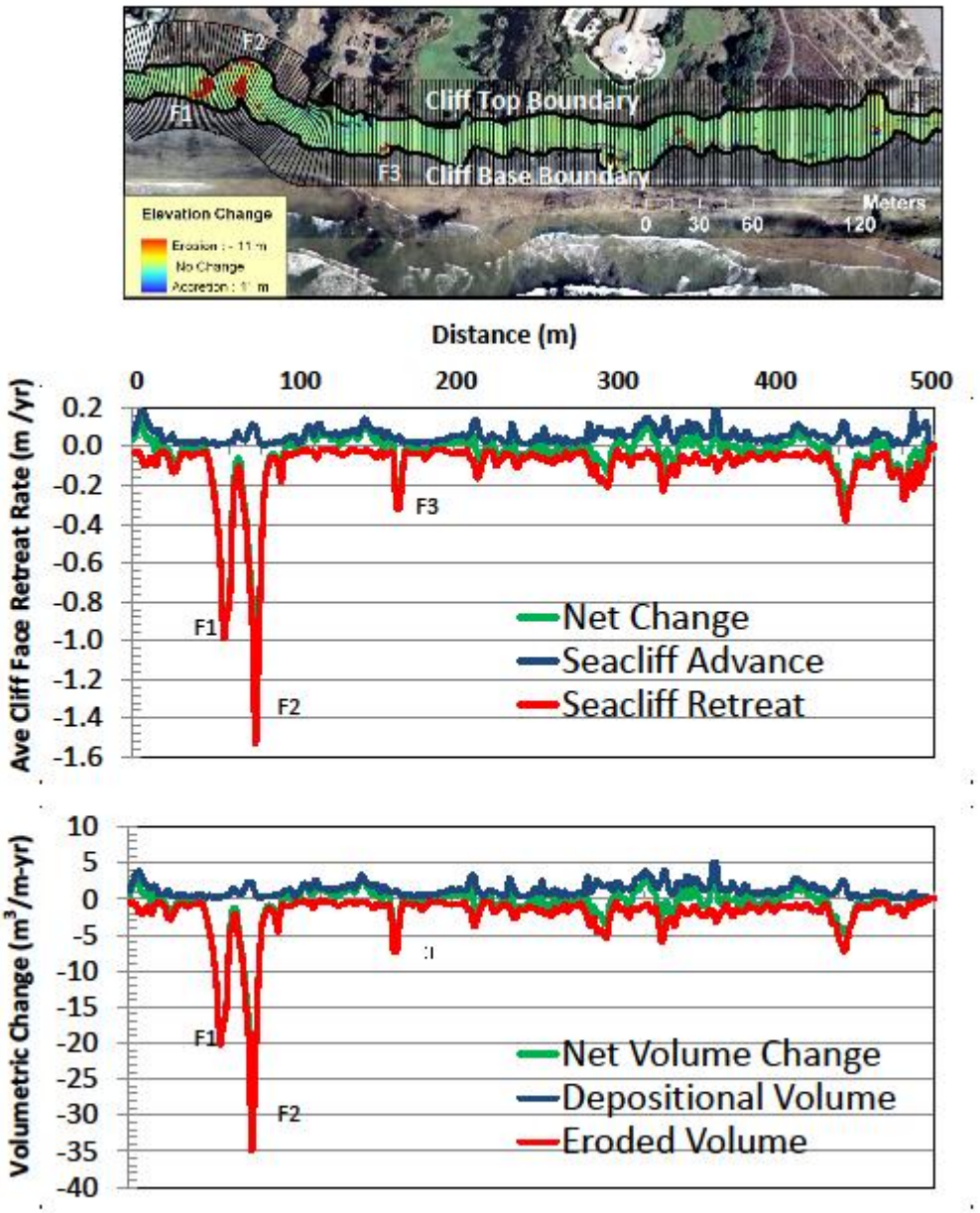

599

600 **Figure 6 – Elevation change grid and compartment analysis for Case Study #1 (October**
601 **2005 – March 2007), showing results for net, erosion, and accretion change. Note that most**
602 **of the erosion was dominated by 2 failure events (F1 and F2).**

603

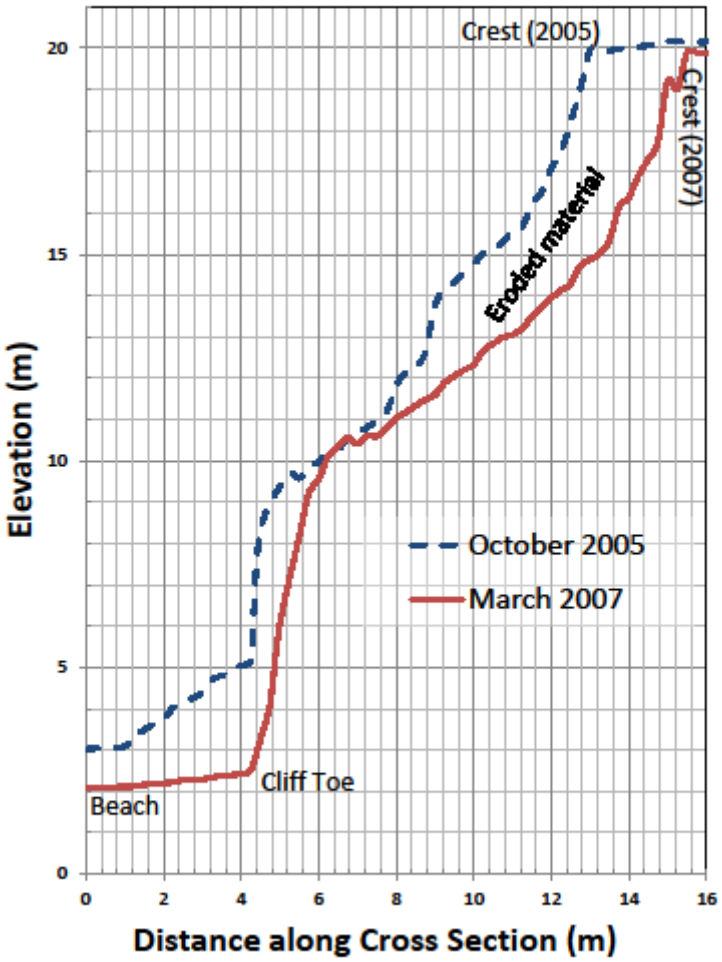

604

605 **Figure 7 – Elevation profiles at site F1 for Case Study #1 (October 2005 and March 2007).**

606

607

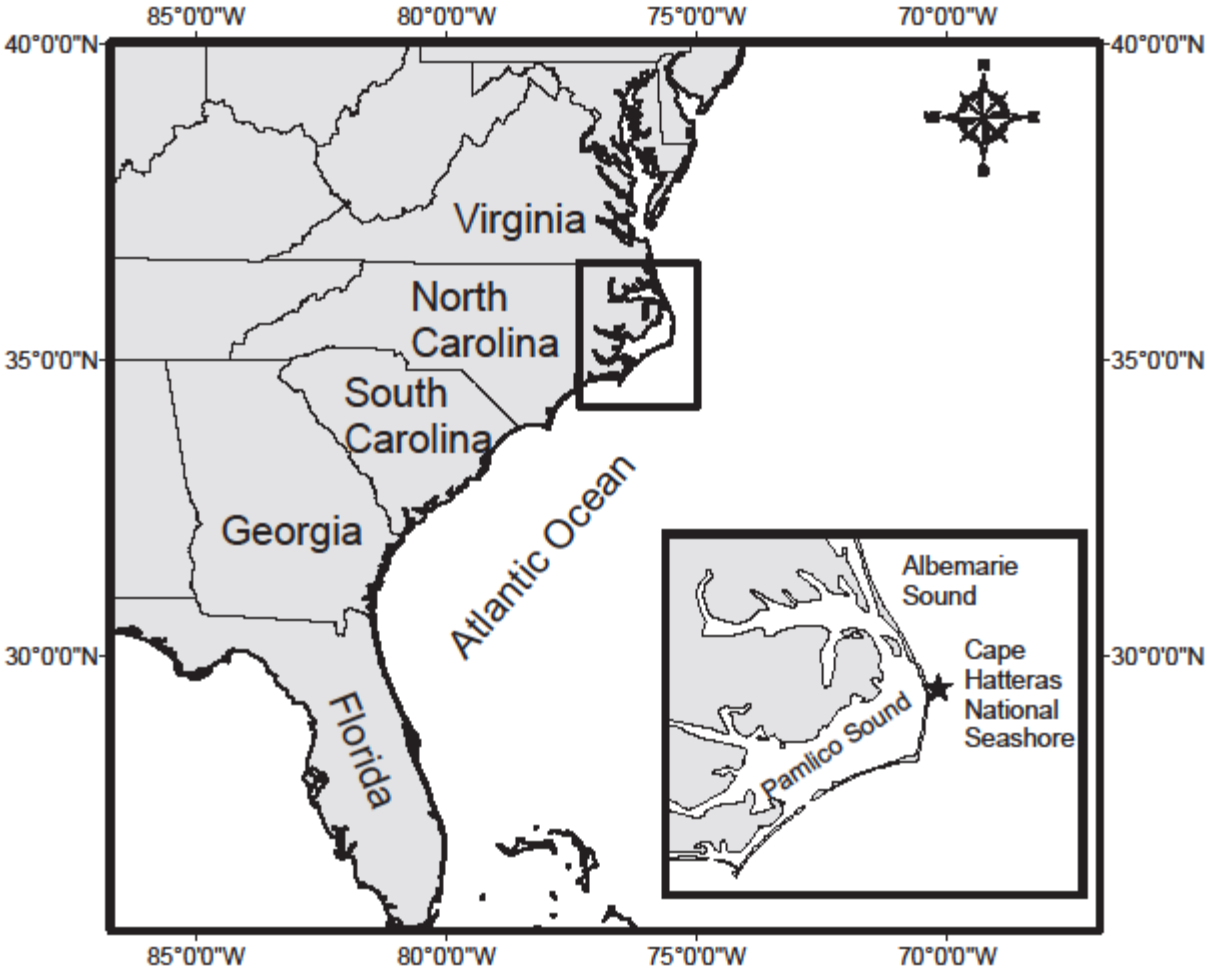

608

609 **Figure 8 - Location Map for Case Study #2 at Cape Hatteras National Seashore, North**

610 **Carolina.**

611

612

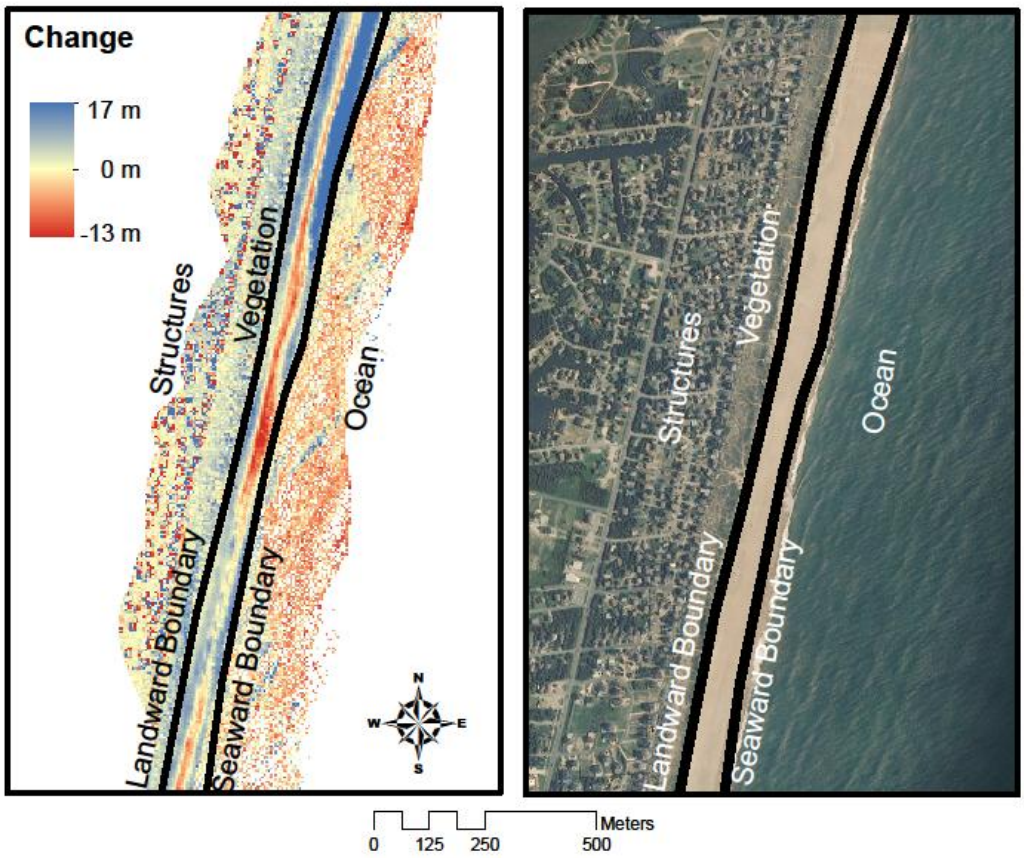

Figure 9 - Analysis boundaries for Cape Hatteras National Seashore, North Carolina showing the manually digitized landward and seaward boundaries using the change grid and aerial photography as a guide. Note the speckled appearance over the ocean due to wave movement during the scan. Also, the photograph was not taken at the exact same time as the scans; hence the water's edge cannot be digitized from it.

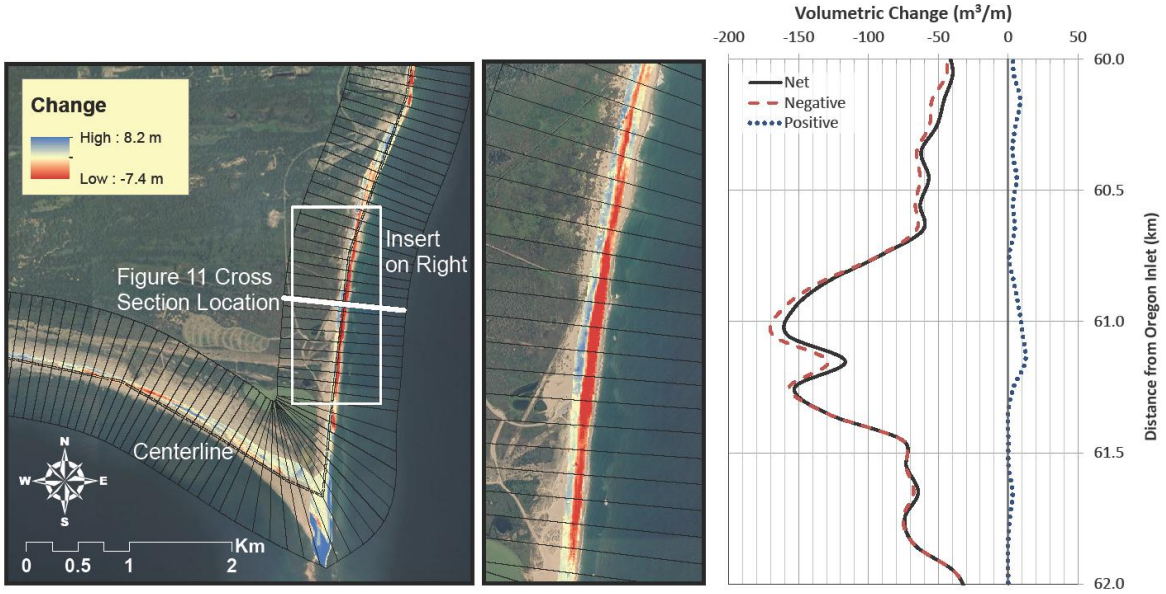

621
622 **Figure 10. Left: Compartmentalization of a section of the study area. The centerline is**
623 **shown as double dashed lines. Note the significant accretion at the Cape. Right: Change**
624 **analysis for a 2km section showing dominant erosion compared to accretion.**

625

626

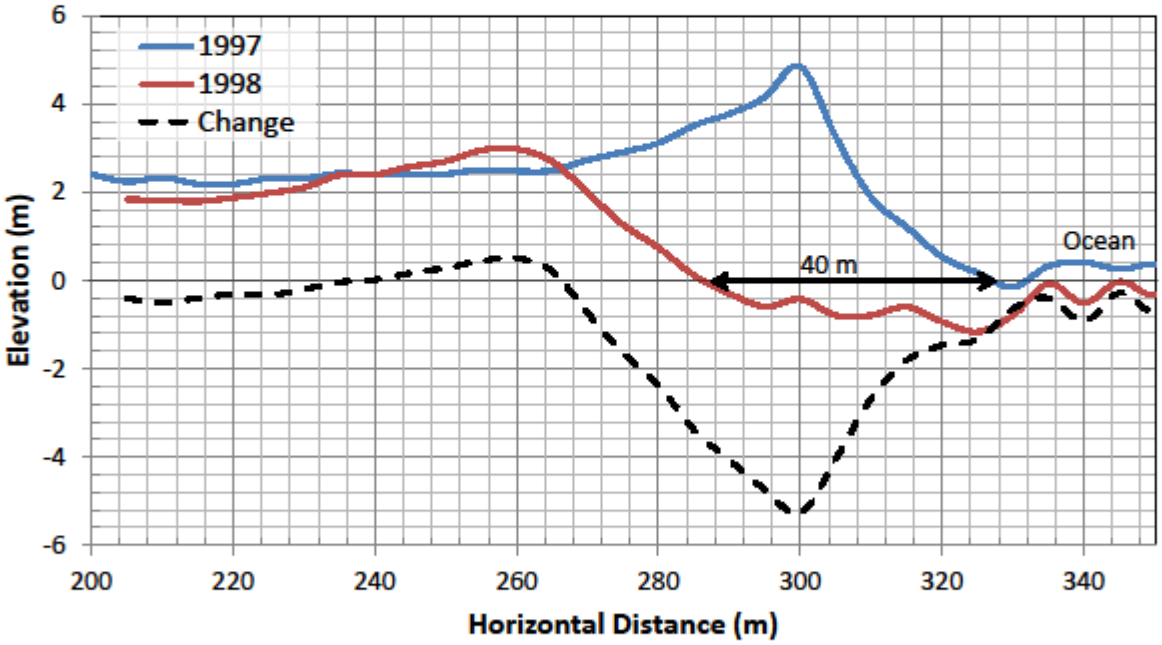

Figure 11. Cross section approximately 2.4 km north from Cape Hatteras, highlighting differences between the 1997 and 1998 DEMs. The dashed line represents elevation differences.